Andreas Almqvist
Associate Professor
Machine Elements,
Luleå University of Technology,
Luleå 97187, Sweden
e-mail: andreas.almqvist@ltu.se

John Fabricius
Assistant Professor
Mathematics,
Luleå University of Technology,
Luleå 97187, Sweden
e-mail: john.fabricius@ltu.se

Roland Larsson
Professor
Machine Elements,
Luleå University of Technology,
Luleå 97187, Sweden
e-mail: roland.larsson@ltu.se

Peter Wall
Professor
Mathematics,
Luleå University of Technology,
Luleå 97187, Sweden
e-mail: peter.wall@ltu.se

A New Approach for Studying Cavitation in Lubrication

The underlying theory, in this paper, is based on clear physical arguments related to conservation of mass flow and considers both incompressible and compressible fluids. The result of the mathematical modeling is a system of equations with two unknowns, which are related to the hydrodynamic pressure and the degree of saturation of the fluid. Discretization of the system leads to a linear complementarity problem (LCP), which easily can be solved numerically with readily available standard methods and an implementation of a model problem in MATLAB *code is made available for the reader of the paper. The model and the associated numerical solution method have significant advantages over today's most frequently used cavitation algorithms, which are based on Elrod–Adams pioneering work.* [DOI: 10.1115/1.4025875]

Keywords: cavitation, tribology, lubrication, linear complementarity problem

1 Introduction

Recently, a very elegant method considering cavitation in hydrodynamic lubrication, was presented by Giacopini et al. [1]. Their model considers the flow in the full film zones as incompressible, it is mass conserving and after discretization the system becomes a LCP. It is a reformulation of the model presented by Bayada et al. [2,3], which can be interpreted as a theoretical representation of the cavitation algorithm presented by Elrods [4]. Existence and uniqueness of the solution follows by the rigorous mathematical analysis in Bayada et al. [5]. The advantage with the reformulation is that the two unknowns become complementary throughout the whole domain. This is the key that enables the LCP formulation of the discretized system. The advantage with the LCP formulation is that standard techniques can be used to solve the problem numerically, e.g., Lemke's pivoting algorithm, see, e.g., the book by Cottle et al. [6]. This alleviates the problems associated with discrete formulations that changes at the boundaries between the cavitated and the full film zones. Moreover, this solution technique finds the solution in a finite number of steps; hence issues related to iterative processes are avoided.

Elrods and Adams [7], proposed another model for analyzing cavitation in hydrodynamic lubrication. These ideas where further developed by Vijayaraghavan and Keith [8]. Contrary to the model in Ref. [2], the lubricant is assumed to be compressible in the full film phase. More precisely, in Refs. [7,8], the lubricant is assumed to obey the compressibility condition

$$\rho = \rho_c \exp((p - p_c)/\beta) \tag{1}$$

where ρ is the lubricant density, p is the pressure, ρ_c is the density at cavitation pressure p_c, and β is the bulk modulus of the lubricant. Like Elrod, they presented a so called "universal equation" in which the dimensionless density (or saturation) ρ/ρ_c, is the single unknown.

Contributed by the Tribology Division of ASME for publication in the JOURNAL OF TRIBOLOGY. Manuscript received June 17, 2013; final manuscript received October 24, 2013; published online November 20, 2013. Assoc. Editor: Daniel Nélias.

During the review process of this paper, it came to the authors' knowledge that an interesting paper by Bertocci et al. [9] will be published in Tribology International, Vol. 67, November, 2013. They present a cavitation model considering compressible fluids. Like in the work by Sahlin et al. [10], it is capable of considering nonlinear pressure-density relationships. The modeling in Ref. [9] results in a complementarity formulation, whereas in Ref. [10], a so called switch function is introduced. Both approaches leads to nonlinear systems of equations that require iterative solution procedures.

The present model is based on the constant bulk modulus compressibility formulation. A change of variables is introduced in the derivation that leads to linear complementarity problem not requiring an iterative solution process. One of the novelties of the present work is that the derivation of the model starts from an expression for the mass flow, which leads directly to a linear complementarity formulation. This is in contrast to Ref. [1] (and Ref. [9]) where the pressure–density relationship is inserted directly into the Reynolds equation and after some argumentation (avoided in the present approach) supporting the cancellation of a term that finally leads to their complementarity formulation.

It should be noted that the analysis presented here can be applied to derive a cavitation model, including all the same features as in Ref. [9]. The procedure would then be to start from Eq. (3), assuming the viscosity μ to be a function of the pressure p and by incorporating a generalization of Eq. (1), i.e.

$$\rho = \rho_c f(p) \tag{2}$$

where $f(p)$ is representing an arbitrary pressure–density relationship. In this case, the final problem will be nonlinear and require an iterative solution procedure.

The reason for choosing to study the constant bulk modulus case in this work is to enable the change of variables that leads to a linear complementarity formulation. The analytical solution for a one-dimensional pocket bearing is derived here, against which the numerical results are validated. In another numerical example, it is shown that the solution corresponding to an incompressible fluid is obtained in the limit as the bulk modulus β goes to infinity, as expected. The numerical solution of the proposed model is also compared to the solution obtained in Ref. [10], for a double parabolic slider geometry. Such a comparison is also conducted in the forthcoming paper [9], by the application of their iterative method. Moreover, some important aspects concerning the discretization of the problem are discussed and an implementation of a model problem in MATLAB code is made available for the reader (see Ref. [11]).

2 Mathematical Model

In this section, a model considering cavitation in thin film flow between two surfaces in relative motion is developed. The surfaces are separated by the distance h, i.e., the film thickness and for simplicity it is assumed that one of the surfaces is stationary and the other one moves with velocity U. The flow is regarded as compressible, according to the density pressure relation in Eq. (1), and the fluid as Newtonian having viscosity μ. Under the presumed conditions, the mass flow, q, can be modeled by

$$q = \frac{\rho h}{2}U - \frac{\rho h^3}{12\mu}\nabla p \tag{3}$$

where both ρ and p are unknowns in the present analysis.

A fluid cannot sustain large tensile stress and in reality, when a liquid is exerted to too high tensile stress cavitation inception occurs. This happens when the pressure falls to the cavitation pressure p_c, i.e., a pressure lower than the saturated vapor pressure. In areas where cavitation takes place, the fluid will be a mixture of liquid and gas bubbles (cavities) and the pressure is more or less constant, i.e., $p \approx p_c$.

The pressure solution given by the Reynolds equation (expressed in its most fundamental form)

$$\nabla \cdot q = 0 \tag{4}$$

may well be below p_c. This calls for an extension of the mathematical model. In fact, this is the main focus of this paper. In the full film zones, the density can be expressed as in Eq. (1). However, in the cavitation zones, the density, or the saturation, is an unknown, denoted here by δ, hence

$$\rho(p) = \rho_c \begin{cases} e^{(p-p_c)/\beta}, & p > p_c \\ \delta, & p = p_c \end{cases} \tag{5}$$

The unknown saturation function δ satisfies $0 \le \delta \le 1$. Since $\nabla p = 0$ in the region where $p = p_c$, we have that

$$q = \rho_c \begin{cases} \dfrac{e^{(p-p_c)/\beta}h}{2}U - \dfrac{e^{(p-p_c)/\beta}h^3}{12\mu}\nabla p, & p > p_c \\ \dfrac{\delta h}{2}U, & p = p_c \end{cases} \tag{6}$$

which is a nonlinear expression in p. It is, however, possible to transform it into a linear expression. Indeed, by introducing the following change of variables

$$u = e^{(p-p_c)/\beta} - 1, u \ge 0 \tag{7}$$

we get that

$$q = \rho_c \begin{cases} \dfrac{uh}{2}U + \dfrac{h}{2}U - \dfrac{\beta h^3}{12\mu}\nabla u, & u > 0 \\ \dfrac{\delta h}{2}U, & u = 0 \end{cases} \tag{8}$$

A key point in the derivation of the present cavitation model is to rewrite this expression by introducing a new unknown variable, η, which is complementary to u in the whole domain, i.e., $u\eta = 0$. The variable η is defined as

$$\eta = 1 - \delta = \begin{cases} 0, & u > 0 \\ 1 - \delta, & u = 0 \end{cases} \tag{9}$$

This means that, if $u > 0$ then $\eta = 0$, and if $u = 0$, then $0 \le \eta \le 1$. The expression for the mass flow in Eq. (8) can now be rewritten as

$$q = \rho_c \begin{cases} \dfrac{hu}{2}U + \dfrac{h}{2}U - \dfrac{\beta h^3}{12\mu}\nabla u, & u > 0 \\ \dfrac{h}{2}U - \dfrac{\eta h}{2}U, & u = 0 \end{cases}$$

alternatively,

$$q = \rho_c \left(\frac{hu}{2}U + \frac{h}{2}U - \frac{\beta h^3}{12\mu}\nabla u - \frac{\eta h}{2}U \right), \quad u \ge 0 \tag{10}$$

Preservation of mass flow is ensured by inserting this for q into the continuity equation, which then reads

$$\nabla \cdot q = \rho_c \nabla \cdot \left(\frac{hu}{2}U + \frac{h}{2}U - \frac{\beta h^3}{12\mu}\nabla u - \frac{\eta h}{2}U \right) = 0$$

Summing up, the following mass preserving cavitation model has been obtained:

$$\begin{aligned} &\nabla \cdot \left(\frac{\beta h^3}{12\mu}\nabla u - \frac{hu}{2}U \right) = \nabla \cdot \left(\frac{h}{2}U \right) - \nabla \cdot \left(\frac{\eta h}{2}U \right) \\ &u \ge 0, \quad 0 \le \eta \le 1, \quad u\eta = 0 \end{aligned} \tag{11}$$

This system allows for a subsequent numerical LCP analysis and when the solution (u, η) has been obtained the fluid pressure p and the saturation δ can be found from Eqs. (7) and (9). For numerical purposes, it is an advantage to use the formulation involving η instead of δ since u and η are complementary throughout the whole domain.

It should be noted that the proposed model can easily be generalized to include the situation where the distance between the surfaces varies with time. The reason for confining the present analysis to the steady state is to avoid obscuring the main ideas with technicalities.

By varying the bulk modulus, the compressibility of the lubricant is varied. A low value of the bulk modulus corresponds to a highly compressible lubricant, while a high value corresponds to a nearly incompressible lubricant. In fact, in the limit $\beta \to \infty$, the present model becomes

$$\begin{aligned} &\nabla \cdot \left(\frac{h^3}{12\mu}\nabla p \right) = \nabla \cdot \left(\frac{h}{2}U \right) - \nabla \cdot \left(\frac{\eta h}{2}U \right) \\ &p \ge 0, \quad 0 \le \eta \le 1, \quad p\eta = 0 \end{aligned} \tag{12}$$

which is a model for the situation when the lubricant is assumed to be incompressible in the full film regions. This means that, by choosing a large value of β, the present model can be used to obtain the pressure solution to the cavitation algorithm proposed in Ref. [1] and a numerical example that demonstrates this fact is presented in Sec. 5.2. It should be remarked that the system in Eq. (12) can also be obtained by starting from the assumption $\rho = \rho_c$ and thereafter following the procedure presented above.

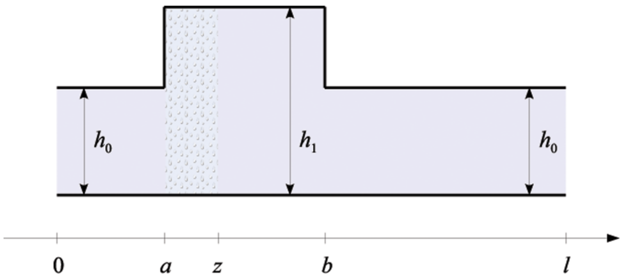

Fig. 1 Schematic illustration of the modeled pocket bearing

3 Analytical Solution

In order to verify the numerical method, a model problem consisting of a one-dimensional pocket slider bearing for which the analytical solution can be derived is considered here. Assume that

$$h(x) = \begin{cases} h_0 & 0 \le x \le a \\ h_1 & a < x < b \\ h_0 & b \le x \le l \end{cases} \tag{13}$$

for which a graphical representation is presented in Fig. 1. An analytical solution to this type of pocket bearing, but assuming an incompressible lubricant, has previously been presented in Ref. [12] (see, also, Ref. [13]).

In this case, the continuity equation becomes one-dimensional and reads

$$\frac{dq}{dx} = \rho_c \frac{d}{dx}\left(\frac{hu}{2}U + \frac{h}{2}U - \frac{\beta h^3}{12\mu}\frac{du}{dx} - \frac{\eta h}{2}U\right) = 0$$

Assuming the boundary conditions

$$p(0) = p_{\text{in}} \quad \text{and} \quad p(l) = p_{\text{out}}$$

for the inlet and outlet, respectively, the cavitation model can be formulated as

$$\begin{aligned} &\frac{d}{dx}\left(\frac{\beta h^3}{12\mu}\frac{du}{dx} - \frac{U}{2}hu\right) = \frac{U}{2}\frac{dh}{dx} - \frac{U}{2}\frac{d}{dx}(\eta h) \\ &u \ge 0, \quad 0 \le \eta \le 1, \quad u\eta = 0 \end{aligned} \tag{14}$$

In order to obtain an analytical solution, it is assumed that the fluid cavitates inside the pocket between the point of rupture at $x = a$ and the point of reformation at $x = z$, where $a \le z \le b$. This means that the bearing can be subdivided into three liquid phase zones; $0 \le x \le a$ and $z \le x \le b$ and $b \le z \le l$ and one gas phase zone $a \le x \le z$, where $u = 0$ and $0 \le \eta \le 1$ In each of the liquid phase zones, $\eta = 0$ and u is given by

$$\frac{d}{dx}\left(\frac{\beta h^3}{12\mu}\frac{du}{dx} - \frac{U}{2}hu\right) = \frac{U}{2}\frac{dh}{dx}$$

Summing up, for each of the zones, the solution explicitly reads

$$u = C_1 + C_2 \exp\left(\frac{6\mu U}{\beta h_0^2}x\right), \quad \eta = 0, \quad 0 \le x \le a \tag{15}$$

$$u = 0, \quad \eta = C, \quad a \le x \le z \tag{16}$$

$$u = C_3 + C_4 \exp\left(\frac{6\mu U}{\beta h_1^2}x\right), \quad \eta = 0, \quad z \le x \le b \tag{17}$$

$$u = C_5 + C_6 \exp\left(\frac{6\mu U}{\beta h_0^2}x\right), \quad \eta = 0, \quad b \le x \le l \tag{18}$$

The boundary conditions

$$u(0) = e^{(p_{\text{in}} - p_c)/\beta} - 1 \quad \text{and} \quad u(a) = 0$$

can be used to determine the constants C_1 and C_2, which then becomes

$$C_1 = -\frac{1 - \exp((p_{\text{in}} - p_c)/\beta)}{1 - \exp\left(-\frac{6\mu U a}{\beta h_0^2}\right)} \tag{19}$$

$$C_2 = -C_1 \exp\left(-\frac{6\mu U a}{\beta h_0^2}\right) \tag{20}$$

The solution u can be used to equate the mass flow

$$q = \frac{\rho_c U h_0}{2}\left(1 - \frac{1 - \exp((p_{\text{in}} - p_c)/\beta)}{1 - \exp\left(-\frac{6\mu U a}{\beta h_0^2}\right)}\right) \tag{21}$$

The mass flow is preserved throughout the whole domain, and according to Eq. (10), the mass flow in $a < x < z$ is given by

$$q = \frac{\rho_c U h_0}{2}(1 - C) \tag{22}$$

which can be used to determine the constant C. That is

$$C = \frac{1 - \exp((p_{\text{in}} - p_c)/\beta)}{1 - \exp\left(-\frac{6\mu U a}{\beta h_0^2}\right)} (= -C_1)$$

The remaining constants C_i, $i = 3, \ldots, 6$ and z, can be found by using the conditions that both the solution and the mass flow are continuous at $x = z$ and $x = b$ and the boundary condition $u(l) = e^{(p_{\text{out}} - p_c)/\beta} - 1$. Summing up

$$C_3 = \frac{h_0}{h_1}(1 - C) - 1 \tag{23}$$

$$C_5 = -C \tag{24}$$

$$C_6 = \frac{\exp((p_{\text{out}} - p_c)/\beta) - 1 - C_5}{\exp\left(\frac{6\mu U l}{\beta h_0^2}\right)} \tag{25}$$

$$C_4 = \frac{-C_3 + C_5 + C_6 \exp\left(\frac{6\mu U b}{\beta h_0^2}\right)}{\exp\left(\frac{6\mu U b}{\beta h_1^2}\right)} \tag{26}$$

and (if it exists) the point of reformation reads

$$z = \frac{\beta h_1^2}{6\mu U}\ln\left(-\frac{C_3}{C_4}\right) - a \tag{27}$$

4 Numerical Solution Procedure

In this section, we will discuss how to discretize the cavitation model in Eq. (11) such that the discretized problem is on the form of a standard linear complementary problem (LCP). Although a two-dimensional formulation is straight forward, a one-dimensional version is presented here in order not to complicate the notation unnecessarily. Two different types of differencing schemes are discussed. In the first type, central and upwind differencing is combined, while the second type is based on central differences only.

4.1 Combined Central and Upwind Differencing. Let us recall the one-dimensional form of in Eq. (11)

$$\frac{d}{dx}\left(a\frac{du}{dx}+bu\right)=\frac{dF}{dx}-\frac{d}{dx}(\eta F) \qquad u\ge 0,\quad 0\le\eta\le 1,\quad u\eta=0 \tag{28}$$

where

$$a=\frac{\beta h^3}{12\mu},\quad b=-\frac{U}{2}h,\quad F=\frac{U}{2}h \tag{29}$$

The problem is discretized using finite differences by dividing the domain $0<x<l$ into a uniform grid with N elements of size $\Delta x=l/N$. Note that, by interpreting u as pressure and choosing coefficients as

$$a=\frac{h^3}{12\mu},\quad b=0,\quad F=\frac{U}{2} \tag{30}$$

the model obtained corresponds to the one presented in Ref. [1], where the lubricant is assumed to be incompressible in the full film regions. The following notation is adopted $x_i=il/N$, where $i=0,\dots,N$ and

$$u_i:=u(x_i)$$

The problem at hand is elliptic in the full film domain, where $\eta=0$. A central difference scheme is therefore used to approximate the derivatives in Eq. (28). If we use the notation

$$a_{i\pm1/2}=\frac{a_{i\pm1}+a_i}{2}$$

and the approximation

$$\left.\frac{du}{dx}\right|_{i+1/2}\approx\frac{u_{i+1}-u_i}{\Delta x}\quad\text{and}\quad\left.\frac{du}{dx}\right|_{i-1/2}\approx\frac{u_i-u_{i-1}}{\Delta x}$$

we obtain

$$\frac{d}{dx}\left(a\frac{du}{dx}+bu\right)\approx\frac{a_{i+1/2}\left.\frac{du}{dx}\right|_{i+1/2}-a_{i-1/2}\left.\frac{du}{dx}\right|_{i-1/2}}{\Delta x}+\frac{(bu)_{i+1}-(bu)_{i-1}}{2\Delta x}$$

$$\approx\frac{\left(\frac{a_{i+1}+a_i}{2}\right)\left(\frac{u_{i+1}-u_i}{\Delta x}\right)-\left(\frac{a_{i-1}+a_i}{2}\right)\left(\frac{u_i-u_{i-1}}{\Delta x}\right)}{\Delta x}+\frac{b_{i+1}u_{i+1}-b_{i-1}u_{i-1}}{2\Delta x}$$

$$=\frac{1}{2\Delta x^2}[(a_{i-1}+a_i)u_{i-1}-(a_{i-1}+2a_i+a_{i+1})u_i+(a_i+a_{i+1})u_{i+1}]+\frac{b_{i+1}u_{i+1}-b_{i-1}u_{i-1}}{2\Delta x}$$

for the left hand side. The first term in the right hand side becomes

$$\frac{dF}{dx}\approx\frac{F_{i+1}-F_{i-1}}{2\Delta x}$$

In the cavitated regions, where $u=0$, we observe that the equation is hyperbolic in η and an upwind difference scheme is employed accordingly, i.e.,

$$\frac{d}{dx}(\eta F)\approx\frac{\eta_iF_i-\eta_{i-1}F_{i-1}}{\Delta x}$$

Let us introduce the following notation

$$\begin{aligned}c_i&=\frac{a_{i-1}+a_i}{2\Delta x^2}-\frac{b_{i-1}}{2\Delta x}\\ d_i&=-\frac{a_{i-1}+2a_i+a_{i+1}}{2\Delta x^2}\\ e_i&=\frac{a_i+a_{i+1}}{2\Delta x^2}+\frac{b_{i+1}}{2\Delta x}\\ z_i&=\frac{F_{i+1}-F_{i-1}}{2\Delta x}\\ g_i&=-\frac{F_i}{\Delta x}\\ k_i&=\frac{F_{i-1}}{\Delta x}\end{aligned}$$

Using this notation, we define the following matrices and vectors

$$A=\begin{bmatrix} d_1 & e_1 & 0 & 0 & 0 & \cdots & & \\ c_2 & d_2 & e_2 & 0 & 0 & \cdots & & \\ 0 & c_3 & d_3 & e_3 & 0 & \cdots & & \\ \vdots & \vdots & \ddots & \ddots & \ddots & & & \\ & & & \ddots & \ddots & \ddots & & \\ & & & & \ddots & \ddots & \ddots & \\ & & & & & c_{N-2} & d_{N-2} & e_{N-2} \\ & & & & & 0 & c_{N-1} & d_{N-1}\end{bmatrix} \tag{31}$$

$$f=\begin{bmatrix} z_1-c_1u_0-k_1\eta_0 \\ z_2 \\ z_3 \\ \\ \\ z_{N-2} \\ z_{N-1}-e_{N-1}u_N\end{bmatrix} \tag{32}$$

where the values of η on the boundaries are computed from the complementarity conditions $u_0\eta_0=0$ and $u_N\eta_N=0$, and

$$B=\begin{bmatrix} g_1 & 0 & 0 & 0 & 0 & \cdots & & \\ k_2 & g_2 & 0 & 0 & 0 & \cdots & & \\ 0 & k_3 & g_3 & 0 & 0 & \cdots & & \\ \vdots & \vdots & \ddots & \ddots & & & & \\ & & & \ddots & \ddots & & & \\ & & & & \ddots & \ddots & & \\ & & & & & k_N & g_{N-2} & 0 \\ & & & & & 0 & k_{N-1} & g_{N-1}\end{bmatrix} \tag{33}$$

The discretized form of Eq. (14) can now be written as

$$Au=f+B\eta,\quad u_i,\eta_i\ge 0,\quad u_i\eta_i=0 \tag{34}$$

Solving this system for u gives

Table 1 Input parameters for the pocket bearing problem

a	b	l	h_0	h_1	p_c	U	μ	$p_{\text{in}} = p_{\text{out}}$
2 mm	5 mm	20 mm	1 μm	10 μm	0 Pa	1 m/s	0.01 Pa s	100 kPa

$$u = q + M\eta, \quad u_i, \eta_i \geq 0, \quad u_i\eta_i = 0 \tag{35}$$

where $q = A^{-1}f$ and $M = A^{-1}B$.

The linear complementarity problem in Eq. (35) can readily be solved by employing standard numerical methods. One which is frequently used is Lemke's pivoting algorithm (see Ref. [6]). One advantage is that Lemke's pivoting algorithm finds the solution in a finite number of steps. Hence, the solution obtained is numerically exact. The method chosen for the present work is a vectorized MATLAB version of a pivoting algorithm solving linear complementarity problems [11].

Note that in the Lemke algorithm, it is not explicitly stated that $\eta_i \leq 1$. However, by using the same ideas as in Ref. [2], it can be proved that any solution to Eq. (11), with Dirichlet boundary conditions, without the condition $\eta \leq 1$ still satisfies $0 \leq \eta \leq 1$. This implies that the numerical solution found with the Lemke algorithm automatically satisfies $\eta_i \leq 1$. This agrees with the physical interpretation that the saturation $(1-\eta)$ must be positive and cannot be larger 1.

4.2 Elliptic Formulation and Central Differencing. In the previous subsection, central differences were used above in the full film region and upwind differences in the cavitated regions. However, it is possible to use central differences throughout the whole domain by introducing a small perturbation, which makes the problem in Eq. (14) elliptic also in η and not only in u. Indeed

$$\begin{aligned} &\frac{d}{dx}\left(a\frac{du^\varepsilon}{dx} + bu^\varepsilon\right) = \frac{dF}{dx} - \frac{d}{dx}\left(\varepsilon\frac{d\eta^\varepsilon}{dx} + \eta^\varepsilon F\right) \\ &u^\varepsilon \geq 0, \quad 0 \leq \eta^\varepsilon \leq 1, \quad u^\varepsilon\eta^\varepsilon = 0 \end{aligned} \tag{36}$$

where $\varepsilon > 0$ is a small parameter. Discretized by central differences, in the same manner as described above, this can be written as

$$Au^\varepsilon = f + (\varepsilon D + B)\eta^\varepsilon, \quad u_i^\varepsilon, \quad \eta_i^\varepsilon \geq 0, \quad u_i^\varepsilon\eta_i^\varepsilon = 0 \tag{37}$$

In order to get the standard form for linear complementarity problems, we can rewrite this as

$$u^\varepsilon = q^\varepsilon + M^\varepsilon\eta^\varepsilon, \quad u_i^\varepsilon, \quad \eta_i^\varepsilon \geq 0, \quad u_i^\varepsilon\eta_i^\varepsilon = 0$$

where

$$q^\varepsilon = A^{-1}f \quad \text{and} \quad M^\varepsilon = A^{-1}(\varepsilon D + B)$$

For small values of ε, u^ε and η^ε in Eq. (36) are good approximations of u and η in Eq. (28). In practice, relatively small means small compared to $(\Delta x)^2$. The idea of adding an extra term is inspired from regularity theory for partial differential equations, which in this context is known as artificial viscosity, see, e.g., Ref. [14].

5 Examples

In this section, the proposed numerical method will be verified. This is done, by first considering a pocket bearing of the type defined in Sec. 3. The main reason for choosing this type of problem is that the analytical solution can be readily obtained. An additional benefit is that this enables a comparison with the results presented in Refs. [1,12], where the same pocket bearing was studied but assuming that the lubricant is incompressible in its full film phase. Additionally, the double parabolic slider model problem investigated in Ref. [10] is analyzed with the two suggested discretization methods presented in Sec. 4.

5.1 Numerical Versus Analytical Solution. In this example, the numerical simulation procedure described above is verified against the analytical solution for the pocket bearing problem in Sec. 3. The selected set of input parameters are presented in Table 1.

Figure 2 depicts the analytical and the numerical pressure solutions for the pocket bearing with input parameters given Table 1. The solutions are obtained for $\beta = 5 \times 10^8$ and $N = 512$. The relative error, defined as

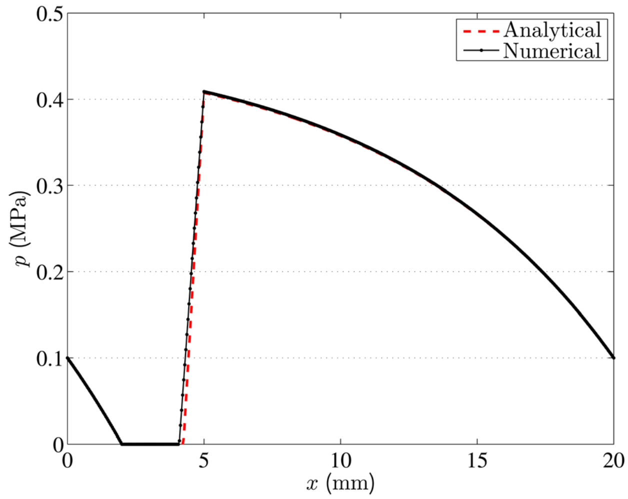

Fig. 2 The analytical and the numerical pressure solutions, for the pocket bearing with input parameters given Table 1, $\beta = 5 \cdot 10^8$ and $N = 512$

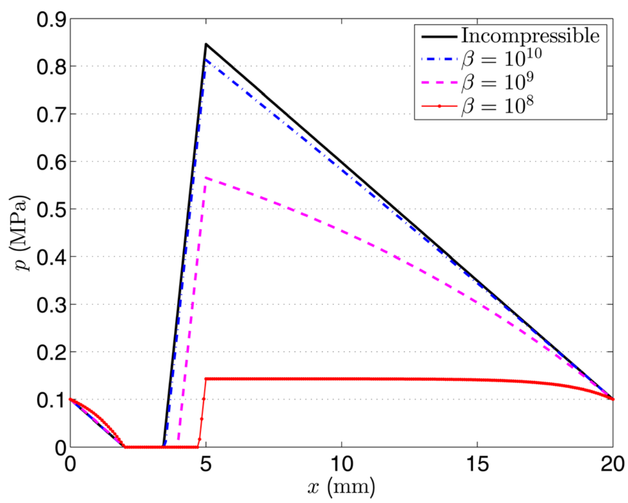

Fig. 3 Influence of the bulk modulus on fluid film pressure

Table 2 Input parameters for the double parabolic slider problem

l	h_0	p_c	U	μ	B	$u(0)$	$u(l)$
76.2 mm	25.4 μm	0 Pa	4.57 m/s	0.039 Pa s	0.069 GPa	0.0001	0

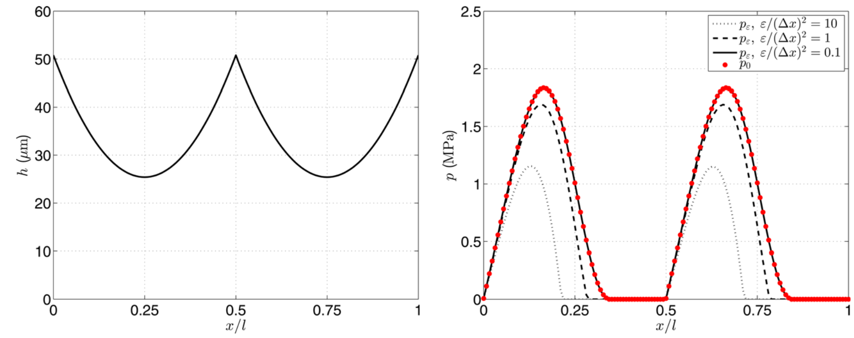

Fig. 4 Double parabolic slider. Geometry (left), pressure distributions (right). p_ε are numerical solutions of Eq. (36) and p_0 is the numerical solution of (28). All solutions are obtained with $N = 128$.

$$\sum_{i=0}^{N}\left|p_i^{\text{analytical}} - p_i^{\text{numerical}}\right| \Bigg/ \sum_{i=0}^{N} p_i^{\text{analytical}}$$

was 6, 2.5, and 1% (and the computational times were 106, 22, and 3 ms on a standard laptop) for $N = 128$, $N = 256$, and $N = 512$, respectively. The numerical difficulties are concentrated to the reformation occurring close to the discontinuity in h.

5.2 Varying the Bulk Modulus β. The degree of compressibility of a lubricant can be described by its bulk modulus β (see Eq. (1)). When the bulk modulus increases, the lubricant will behave more and more like an incompressible fluid. In fact, in the limit as $\beta \to \infty$, the present model in Eq. (11) coincides with Eq. (12), where the lubricant is modeled as incompressible in the full film phase. In Fig. 3, pressure solutions $p(x)$ of the one-dimensional problem in Eq. (28) with coefficients given by Eq. (29) for $\beta = 10^8$ Pa, $\beta = 10^9$ Pa and $\beta = 10^{10}$ Pa are presented together with the solution corresponding to an incompressible lubricant, obtained by solving Eq. (28) with coefficients given by Eq. (30). The numerical results clearly illustrate how the pressure solution of the compressible problem converges towards the solution of the incompressible problem, as the bulk modulus β increases. From the results shown in the figure, it is also suggested that the load carrying capacity of the bearing increases as the compressibility of the fluid decreases. Note that, an analytical solution for an incompressible lubricant was presented in Ref. [12]. The relative difference in mass flow between the inlet and the outlet was evaluated for the numerical solution. The largest difference; $5 \cdot 10^{-7}$ arises for the solution with $\beta = 10^8$.

5.3 A Double Parabolic Slider. In the last example, results obtained with the present method is compared with results presented in Ref. [10]. More precisely, the double parabolic slider geometry that was studied in Ref. [10] is also analyzed here. Both methods proposed in Sec. 4 are used to obtain pressure solutions and the influence of the small parameter ε is studied.

The film thickness h for the double parabolic slider is given by

$$h(x) = h_0 + h_0\left(\frac{4}{l}\right)^2 \begin{cases} \left(x - \frac{l}{4}\right)^2 & 0 \le x \le l/2 \\ \left(x - \frac{3l}{4}\right)^2 & l/2 \le x \le l \end{cases} \tag{38}$$

and the selected set of input data are presented in Table 2.

To the left in Fig. 4, the geometry of the double parabolic slider is depicted. The right hand side of the same figure shows pressure distribution p_0 obtained by solving Eq. (28) and the pressure distributions p_ε obtained by solving Eq. (36) for $\varepsilon = 10(\Delta x)^2$, $\varepsilon = 1(\Delta x)^2$, and $\varepsilon = 0.1(\Delta x)^2$. All solutions are obtained with $N = 128$. It can be seen, that for small values of ε, the two methods coincide numerically. The pressure solutions p_0 and p_ε (for small values of ε) are visually identical to the solution obtained in Ref. [10].

Nomenclature

h = film thickness (m)
p = pressure (Pa)
p_c = cavitation pressure (Pa)
q = mass flow (kg/(ms)))
u = LCP solution variable $u = e^{(p-p_c)/\beta} - 1$
U = velocity of the moving surface (m/s)
β = lubricant bulk modulus (Pa)
δ = saturation function
η = LCP solution variable $\eta = 1 - \delta$
μ = dynamic viscosity (Pas)
∇ = gradient $\nabla = (\partial/\partial x_1, \partial/\partial x_2)$ (1/m)
ρ = lubricant density (kg/m^3)
ρ_c = lubricant density at cavitation pressure (kg/m^3)

References

[1] Giacopini, M., Fowell, M. T., Dini, D., and Strozzi, A., 2010, "A Mass-Conserving Complementarity Formulation to Study Lubricant Films in the Presence of Cavitation," J. Tribol., **132**(4), p. 041702.
[2] Bayada, G., Martin, S., and Vazquez, C., 2005, "Two-Scale Homogenization of a Hydrodynamic Elrod-Adams Model," Asymptotic Anal., **44**(1), pp. 75–110.
[3] Bayada, G., Martin, S., and Vázquez, C., 2005, "An Average Flow Model of the Reynolds Roughness Including a Mass-Flow Preserving Cavitation Model," J. Tribol., **127**(4), pp. 793–802.
[4] Elrod, H. G., 1981, "A Cavitation Algorithm," J. Tribol., **103**, pp. 350–354.
[5] Bayada, G., Talibi, M. E. A., and Hadi, K. A., 2007, "Existence and Uniqueness for a Non-Coercive Lubrication Problem," J. Math. Anal. Appl., **327**, pp. 585–610.
[6] Cottle, R. W., Pang, J. S., and Stone, R. E., 2009, "The Linear Complementarity Problem," Report No. 60, SIAM, Philadelphia, PA.
[7] Elrod, H. G., and Adams, M. L., 1975, "A Computer Program for Cavitation and Starvation Problems," *Cavitation and Related Phenomena in Lubrication*, D. Dowson, M. Godet, and C. M. Taylor, eds., Mechanical Engineering Publications, ITC, Sugar Grove, IL, pp. 37–43.
[8] Vijayaraghavan, D., and Keith, T. G., Jr., 1989, "Development and Evaluation of a Cavitation Algorithm," STLE Tribol. Trans., **32**(2), pp. 225–233.
[9] Bertocchi, L., Dini, D., Giacopini, M., Fowell, M. T., and Baldini, A., 2013, "Fluid Film Lubrication in the Presence of Cavitation: A Mass-Conserving Two-Dimensional Formulation for Compressible, Piezoviscous and Non-Newtonian Fluids," Tribol. Int., **67**, pp. 61–71.
[10] Sahlin, F., Almqvist, A., Larsson, R., and Glavatskih, S., 2007, "A Cavitation Algorithm for Arbitrary Lubricant Compressibility," Tribol. Int., **40**(8), pp. 1294–1300.
[11] Almqvist, A., Spencer, A., and Wall, P., 2013, "Matlab Routines Solving a Linear Complementarity Problem Appearing in Lubrication With Cavitation," http://www.mathworks.com/matlabcentral/fileexchange/41484
[12] Olver, A. V., Fowell, M. T., Spikes, H. A., and Pegg, I. G., 2006, "'Inlet Suction', a Load Support Mechanism in Non-Convergent, Pocketed, Hydrodynamic Bearings," Proc. Inst. Mech. Eng., Part J: J. Eng. Tribol., **220**(2), pp. 105–108.
[13] Fowell, M., Olver, A. V., Gosman, A. D., Spikes, H. A., and Pegg, I., 2007, "Entrainment and Inlet Suction: Two Mechanisms of Hydrodynamic Lubrication in Textured Bearings," J. Tribol., **129**(2), pp. 336–347.
[14] Evans, L. C., 2010, *Partial Differential Equations*, 2nd ed., Vol. 19 of Graduate Studies in Mathematics, American Mathematical Society, Providence, RI.

ERRATUM NOTICE

This paper has been modified since being posted online. The DOI of the published erratum is: 10.1115/4026593

The changes from the erratum are listed below and have been incorporated into this version of the paper.

Typographical Correction
Equation (23), p. 011706–3, incorrectly reads

$$C_3 = \frac{h_0}{h_1}(C - 1)$$

The correct equation is

$$C_3 = \frac{h_0}{h_1}(1 - C) - 1$$

which is also the equation used in the discretized implementation of the analytical solution, which was compared to the numerical one, shown in Fig. 2 on p. 011706–5.